Article published online: 2024-01-16

Original Article

Hemoperitoneum Quantification in Non-contrast CT: Evaluating Feasibility with the Novel HUVAO Segmentation Algorithm

Rahul Bhagawati[1] Suman Hazarika[2] Cota Navin Gupta[1] Souptick Chanda[1,3]

[1] Department of Biosciences and Bioengineering, Indian Institute of Technology Guwahati, North Guwahati, Assam, India
[2] Division of CT, MRI, and Conventional Radiology, Apollo Hospitals Guwahati, Guwahati, Assam, India
[3] Mehta Family School of Data Science and Artificial Intelligence, Indian Institute of Technology Guwahati, North Guwahati, Assam, India

Address for correspondence Rahul Bhagawati, PhD Scholar, Department of Biosciences and Bioengineering, Indian Institute of Technology Guwahati, North Guwahati 781 039, Assam, India (e-mail: r.bhagawati@iitg.ac.in).

J Gastrointestinal Abdominal Radiol ISGAR

Abstract

Background Injuries involving substantial bleeding, frequently encountered in victims of road traffic accidents, pose a significant risk to mortality. For abdominal trauma cases, accurately assessing internal bleeding and hematomas becomes crucial. Detecting hemoperitoneum, which indicates both blood loss and organ damage in the abdominal cavity, requires precise evaluation. Timely diagnosis and quantification of hemoperitoneum following road accidents are crucial during the critical golden hour, enabling prioritized medical intervention and potentially saving lives while enhancing overall patient care. However, achieving precise hemoperitoneum quantification in abdominal trauma faces challenges due to the intricate nature of overlapping Hounsfield unit (HU) regions.

Methods In this feasibility study, we sought to assess the efficacy of the novel *HUVAO* (Hounsfield Unit-based Volume quantification of Asymmetrical Objects) segmentation algorithm for quantifying hemoperitoneum in thoracoabdominal non-contrast computed tomography (CT) images. Using 28 retrospective non-contrast CT scans of thoracoabdominal regions from trauma patients, we analyzed crucial imaging data without necessitating additional scans or contrast-enhanced procedures. The study aimed to compare *HUVAO* against classical algorithms and visual estimations by trained radiologists for hemoperitoneum segmentation in thoracoabdominal non-contrast CT images.

Results Our findings revealed that although the technical feasibility of employing *HUVAO* and other segmentation algorithms for hemoperitoneum quantification is evident, the outcomes derived from these algorithms display notable discrepancies.

Conclusion In assessing technical feasibility, we introduced the *HUVAO* segmentation algorithm for hemoperitoneum quantification, comparing its performance against classical segmentation algorithms and visual estimations from trained radiologists. While our results affirm the technical feasibility of *HUVAO* for this purpose, the observed

Keywords
- hemoperitoneum
- CT scan
- image processing
- Hounsfield units (HU)
- voxel segmentation
- trauma care

DOI https://doi.org/10.1055/s-0043-1778672.
ISSN 2581-9933.

Thieme Medical and Scientific Publishers Pvt. Ltd., A-12, 2nd Floor, Sector 2, Noida-201301 UP, India

variations underscore the task's inherent complexity. This emphasizes the limitations of relying solely on HU-based detection, advocating for integration with clinical data. This insight urges exploration of advanced techniques to boost accuracy and elevate patient care standards.

Introduction

India grapples with the pressing issue of road accidents and the resulting fatalities. It is evidenced by a staggering 168,491 road crash fatalities in 2022, representing a 9% increase from the previous year and an 11.5% increase from 2019, according to the Ministry of Road Transport and Highways' report.[1] This alarming statistic underscores India's ongoing struggle with the critical challenge of road accidents and the loss of lives they entail. Notably, traumatic hemorrhage plays a substantial role in these mortality rates.[2–4] Hence, the timely and precise diagnosis within the critical *golden hour* (the critical time after injury when quick medical care can save lives) becomes pivotal in addressing this issue and saving lives.[5]

Understanding the complexities of hematomas and hemorrhages is paramount in managing injuries and trauma,[6] with particular importance placed on hemoperitoneum,[7] characterized by the accumulation of blood within the abdominal cavity, especially in cases of abdominal trauma.

Diverse tools and imaging techniques are employed for the identification and measurement of hemoperitoneum, encompassing manual inspection, palpation, computed tomography (CT), ultrasound imaging, magnetic resonance imaging, and computer-aided diagnosis systems. Among these, CT scans utilizing Hounsfield units (HUs) to gauge hemoperitoneum[8] are preferred for thoracoabdominal trauma detection due to their superior visualization capabilities.[9–15] They remain indispensable in diagnosing and managing internal bleeding, significantly contributing to treatment planning and informed decision-making processes.[16]

Existing Solutions and Challenges to Hemoperitoneum Diagnosis

Numerous classical image processing algorithms are available to tackle the challenges of achieving accurate segmentation and measuring hemoperitoneum volume. Nonetheless, the existing techniques and algorithms have limitations.

For instance, the *Tada* formula and its adaptations offer a basic estimate suitable for preliminary ellipsoid hemorrhage diagnosis, yet they fall short of accurately measuring sizable and asymmetrical hemorrhage.[17–19] The *Tada* formula's ellipsoid shape assumption has greater validity for the relatively homogeneous and limited cranial space. However, the abdominal cavity exhibits a wider variety of irregular forms and subject-specific variations, which limits its applicability for precise hemoperitoneum volume measurement. Region-based methods such as clustering, region-growing, contour-finding, and active contours rely on user expertise for precise segmentation.[20–26] Consequently, prevalent software packages incorporating classical image processing techniques, including region-growing algorithms, manual approaches, and spline methods, lean on explicit user inputs and offer restricted accuracy.[27–34] Training and validation of statistical models for segmentation demand an extensive data set and manual CT scan segmentation—a task complicated by pixel intensity variations, border intricacies, high-contrast tissues, noise, and anomalies.[35–38]

Moreover, visually inspecting or manually assessing hemoperitoneum CT scans is vulnerable to intra- and inter-rater disparities, arbitrary imprecisions, and misinterpretations, all while consuming valuable time.[39–42] In light of these limitations, there is a clear need for more advanced and accurate approaches to address the complexities of hemoperitoneum diagnosis and segmentation.

Aim and Objective

The primary objective of this study is to retrospectively examine and compare the effectiveness of both novel and classical image processing algorithms in accurately segmenting hemoperitoneum areas in a group of 28 ($n = 28$) thoracoabdominal noncontrast CT images. We introduce *HUVAO* (Hounsfield Unit-based Volume quantification of Asymmetrical Objects), a novel algorithm utilizing region splitting and cluster selection guided by user inputs. We aim to evaluate how efficiently *HUVAO* segments and estimates hemoperitoneum volume. We evaluated its performance against visual estimations by two experienced radiologists and classical image processing techniques like Global Thresholding, Multi-Otsu Thresholding, and the Contour-Finding and Filling algorithm in estimating hemoperitoneum. Throughout our investigation, we aim to determine the accuracy of these algorithms in identifying and characterizing hemoperitoneum, examining their strengths and limitations, and exploring the potential for improving segmentation outcomes.

The study employs a *slice-approach* for hemoperitoneum quantification to achieve accurate volume measurement. The approach involves applying the selected segmentation algorithms to each slice of each CT image. The segmented regions obtained are then integrated to yield a comprehensive volume estimation of the hemoperitoneum. This approach has demonstrated its efficacy in delivering precise and reliable outcomes, irrespective of the shape of the hematoma, effectively minimizing shape-related errors and accounting for irregularities.[34]

Furthermore, the study delves into the intricacies of HU values within personalized imaging. By subjecting a novel algorithm to comparison with classical image processing methods, the study seeks to improve the accuracy and efficiency of hemoperitoneum segmentation. The ultimate aim, achieved through meticulous evaluation and exploration, is to identify the most effective algorithm capable of significantly enhancing diagnostic accuracy and improving patient outcomes, particularly in emergencies.

Methods

Data Description and Analysis

This retrospective study involved 28 patients who underwent non-contrast CT scans targeting the thoracic and abdominal regions. ►**Table 1** outlines the CT parameters encompassing the clinical data set utilized in this study.

The CT scan data set was obtained in the Digital Imaging and Communications in Medicine (DICOM) file format. The MicroDicom v2022.1 viewer (64-bit) software was used to check it at first. This software is meant to handle pixel values and slice metadata in DICOM digital data.

Among the cohort of 28 patients under study, a demographic analysis reveals a gender distribution where merely two individuals were identified as female (7%), contrasting with the predominant male representation comprising the remaining 26 patients (93%), as depicted in ►**Fig. 1**. The age spectrum within this group ranged from 8 to 80 years, with a calculated mean age of 35.9 years and a median age of 34.5 years, as shown in ►**Fig. 2**. All subjects shared a commonality in the causes of their injuries, specifically road traffic accidents, and were presented at the hospital's emergency department within 24 to 48 hours post-trauma.

Two experienced radiologists conducted visual estimations of the hemoperitoneum volume by thoroughly evaluating the CT scan images. Additionally, each radiologist independently reviewed the images and reported the observations regarding the presence and extent of hemoperitoneum. Any differences in their assessments were resolved through collaborative discussions.

Algorithms and Techniques Used

Due to the complex characteristics of the obtained clinical data, which include challenges like overlapping HU regions and the absence of well-defined HU ranges for accurate

Table 1 CT parameters of the study

KVP	120
X-ray tube current	176 mA-s
Exposure Time	320 ms
FOV	0.5100859375\0.5100859375 (0.5100859375 mm per pixel)
Slice thickness	1 mm
Slice gap	0.7 mm for the abdomen 0.5 mm for the thorax
Pitch	0.8
Matrix	512 (rows) * 512 (columns)

Abbreviations: CT, computed tomography; FOV, field of view; KVP, kilovoltage peak.

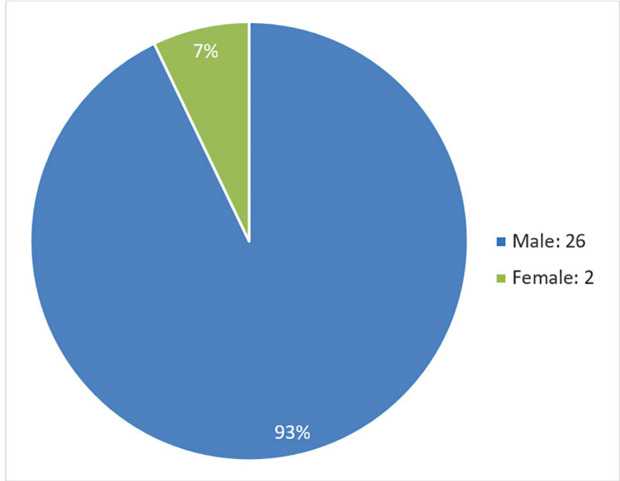

Fig. 1 Gender distribution among the 28 studied patients.

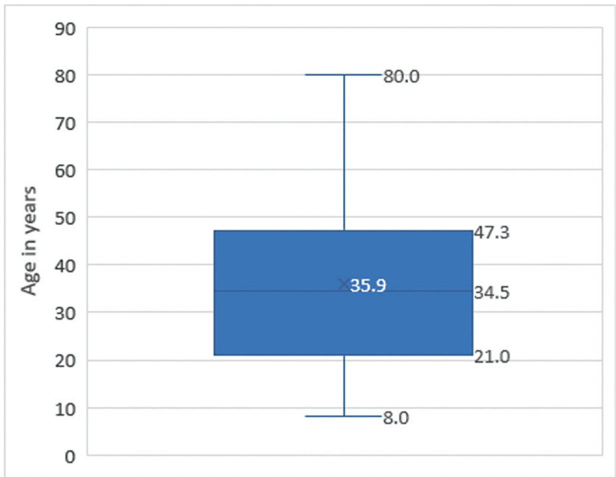

Fig. 2 Age distribution among the 28 studied patients.

hemoperitoneum segmentation, our evaluation encompassed a novel algorithm and a variety of established classical image processing algorithms. The central aim was to segment and quantify hemoperitoneum within the dataset accurately. For a thorough comparison, we treated the mean of hemoperitoneum volume estimates from two radiologists not as a gold standard but as a practical benchmark, representing the "actual or reference value." Visual estimates were used as a reference point for comparison alongside other quantitative methods, not considered the definitive reference value, to ensure a comprehensive evaluation.

The image processing algorithms involved are (1) *HUVAO*, (2) Global Thresholding, (3) Multi-Otsu Thresholding, and (4) Contour-Finding and Filling algorithm. Hemoperitoneum volume quantification adhered to the governing equation below, primarily grounded in the *slice-approach* for hematoma quantification[34]:

$$V_{total} = (\boldsymbol{\Sigma}\, pix) * (l * b * h) * 0.001 \ldots (1)$$

Here, the total estimated volume of the region of interest (ROI) is referred to as "V_{total}," while the CT scan voxel dimensions are denoted as (l, b, h). The term *pix* designates the total count of segmented pixels within a single CT slice along the *XY* axis. The inclusion of the number 0.001 in this formula enables conversion from cubic millimeters to milliliters.

The programming language used in this study is Python 3.8, and the libraries utilized include pydicom, scikit-image, numpy, and others.

HUVAO: the Novel Algorithm

This study introduces *HUVAO*, a novel algorithm that employs region-splitting and cluster-selection techniques guided by user input. *HUVAO* starts by determining the voxel dimensions of the CT scan (l, b, h) and collecting the user-provided predominant HU value (th) within the ROI. For each CT slice, pixel clustering is applied, grouping adjacent pixels with an absolute difference of 1 HU to unite closely related HU values, potentially indicative of the same tissue or structure. This threshold can be adjusted to accommodate different scenarios and user preferences.

After clustering, *HUVAO* receives a range of HU values ($th \pm$ a configurable constant value, e.g., [37 HU $\pm$ 1 HU]) centered around the initial user-provided HU value. Based on the average HU values of the clusters, the algorithm then identifies the clusters that fall within the predefined HU range. The minimum and maximum HU values for each selected cluster are recorded, and the algorithm establishes the final HU range by computing the respective mean of these values. Using the selected range, the algorithm performs a straightforward thresholding process to segment all slices within the ROI, calculating the total count of segmented foreground pixels (*pix*). This information is then used to determine the overall hemoperitoneum volume of one CT scan (V_{total}) following the formulation described in **Eq. 1**. The flowchart depicting *HUVAO* is presented in ►**Fig. 3**.

In the context of this clinical data set, global threshold values for hemoperitoneum segmentation were established through a comprehensive review of relevant literature sources.[43–49] These thresholds, set at 30 HU for the lower limit and 45 HU for the upper limit, were derived from the mode of HU values characterizing unclotted, non-contrast hemoperitoneum, covering both the lower and upper HU ranges. Additionally, when applying *HUVAO* to this data set, a threshold value (th) of 37.5 HU was utilized for hemoperitoneum segmentation. This choice was based on the calculated average between the previously mentioned threshold values of 30 and 45 HU, ensuring a balanced approach in the segmentation process.

Global Thresholding

Global Thresholding is a technique that divides an image into two segments using a single threshold value. Pixels brighter than this threshold are retained, while darker pixels are discarded.[50–52] This method effectively removes the background and facilitates object extraction. In the context of our clinical data set for hemoperitoneum segmentation, global thresholds of 30 and 45 were selected for this algorithm, as detailed in the previous section. The total hemoperitoneum volume of a single CT scan (V_{total}) was determined by utilizing the total count of segmented pixels (*pix*), as outlined in **Eq. 1**.

Multi-Otsu Thresholding

Multi-Otsu Thresholding is a technique that divides an image into multiple classes or segments (default is 3) by determining multiple threshold values based on pixel brightness, effectively categorizing different regions with varying brightness levels.[53–55] In the case of hemoperitoneum segmentation within our clinical dataset, experimentation determined that a minimum of seven classes were needed, and this configuration was adopted. The utilization of seven classes for segmenting the image histogram in each CT scan image led to identifying the optimal thresholding HU values for hemoperitoneum segmentation, precisely 31 (lower HU) and 43 (upper HU). The total number of segmented pixels (*pix*) was then used to find the total hemoperitoneum volume of one CT scan (V_{total}) as described in **Eq. 1**.

Contour-Finding and Filling

The Contour-Finding and Filling algorithm detects constant-value lines within an image but lacks information about the enclosed areas they outline.[24] In the case of CT scans with overlapping HU regions, the algorithm locates the contour coordinates of all the contours present in each CT slice. It involves considering regions with continuous boundaries. Subsequently, the algorithm employs a contour-filling process to fill all the identified contours based on their coordinate information. The algorithm utilizes the previously stated global thresholds (lower average HU = 30, upper average HU = 45) for selection of the filled contours in hemoperitoneum segmentation. The cumulative count of pixels within all the chosen and filled contours constituted the segmented pixels (*pix*). Subsequently, this total count of segmented pixels (*pix*) was used in the calculation of the overall hemoperitoneum volume for a single CT scan (V_{total}), as specified in **Eq. 1**. ►**Fig. 4** provides a visual depiction of the algorithm's workflow.

Results

In this section, we detail the clinical phase of the study, where we performed comprehensive segmentation and volumetric quantification tasks on a Windows 11 AMD Ryzen 7 machine with a 2.3-GHz CPU and 16 GB of RAM. The mean hemoperitoneum volumes, serving as the "actual volumes," were determined through assessments by two radiologists. Several segmentation algorithms were used in the study, such as *HUVAO*, Global Thresholding, Multi-Otsu Thresholding, and Contour-Finding and Filling. ►**Figs. 5** and **6** display the volume estimates generated by each algorithm for all patients, with a deviation plot (the ratio of ("reference volume"/estimated volume) is used to quantify deviation) illustrating variations from the mean (reference) values provided by the clinicians in the cohort.

In terms of computational efficiency, the time complexities of the employed segmentation and quantification algorithms manifest as follows: *HUVAO* exhibited an average

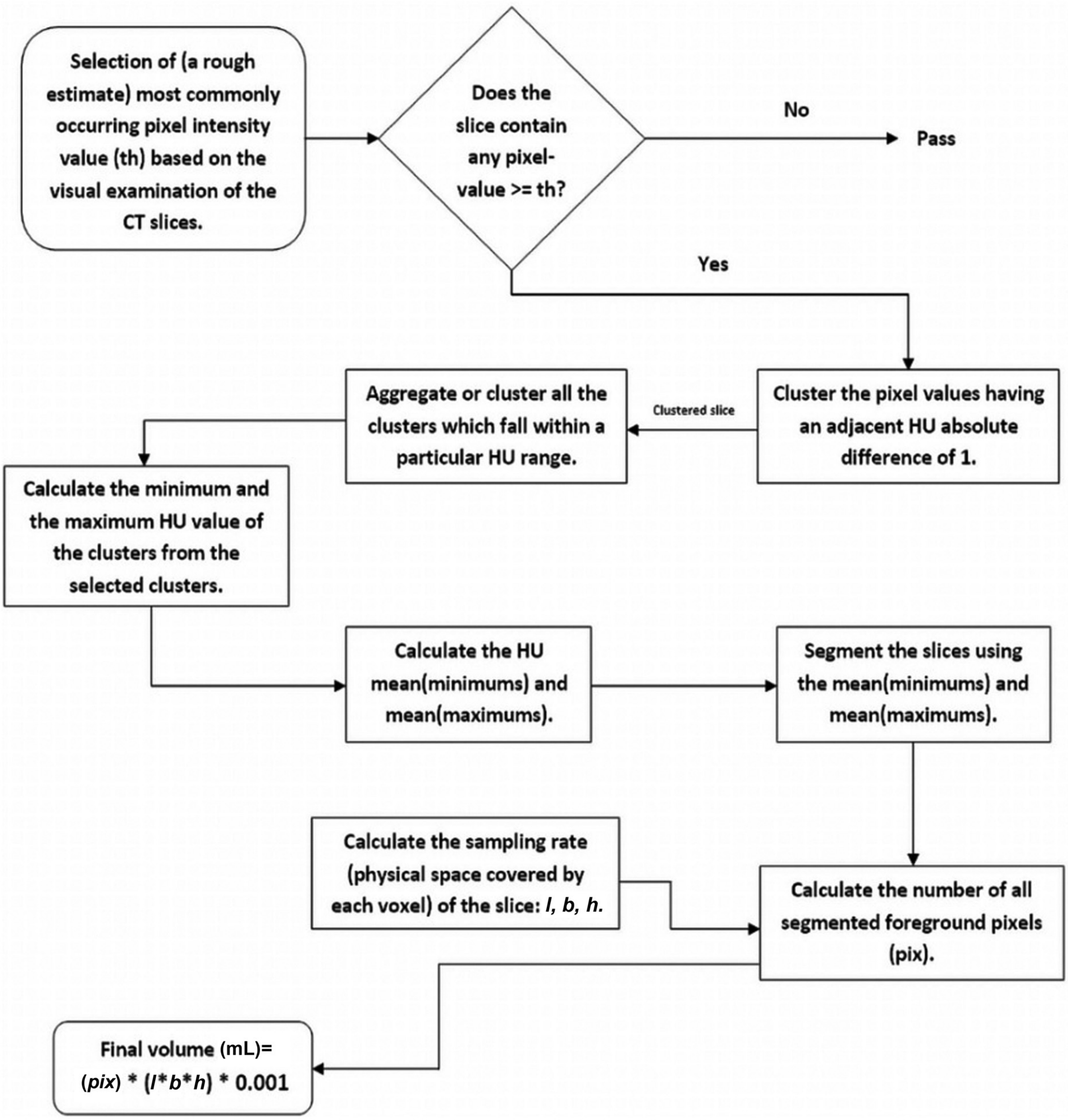

Fig. 3 Segmentation and volume estimation by *HUVAO* (Hounsfield Unit-based Volume quantification of Asymmetrical Objects).

processing time of 10 minutes per CT scan, Global Thresholding took less than 5 seconds per CT scan, Multi-Otsu Thresholding demanded an average processing time of 7 minutes per CT scan, and the Contour-Finding and Filling algorithm had an average processing time of 31 minutes per CT scan.

Discussion

Significant challenges were encountered in the segmentation and volume estimation of the hemoperitoneum in this clinical dataset. These obstacles primarily arose from overlapping HU regions, limited localization precision, and the presence of small hemoperitoneum sizes, collectively complicating the accurate delineation and estimation processes.

Certain methods, like global thresholding and active contour methods, are great for high-contrast images[52] but struggle with overlapping HU regions. Multi-Otsu thresholding needs user inputs like the desired number of classes for image histogram separation[53–55] and does not work well for low contrast and overlapping region segmentation tasks. Clustering algorithms assume well-separated features, impractical for handling overlapping HU regions.[21] Despite being complex, contour-finding algorithm struggles to select suitable thresholds for overlapping areas, impacting accuracy.[24] Region-growing leads to oversegmentation and has specific prerequisites.[22,23] Compared with traditional image processing algorithms, *HUVAO* stands out for its user-friendliness due to minimal user inputs and its ability to deliver promising results, even when dealing with occasional

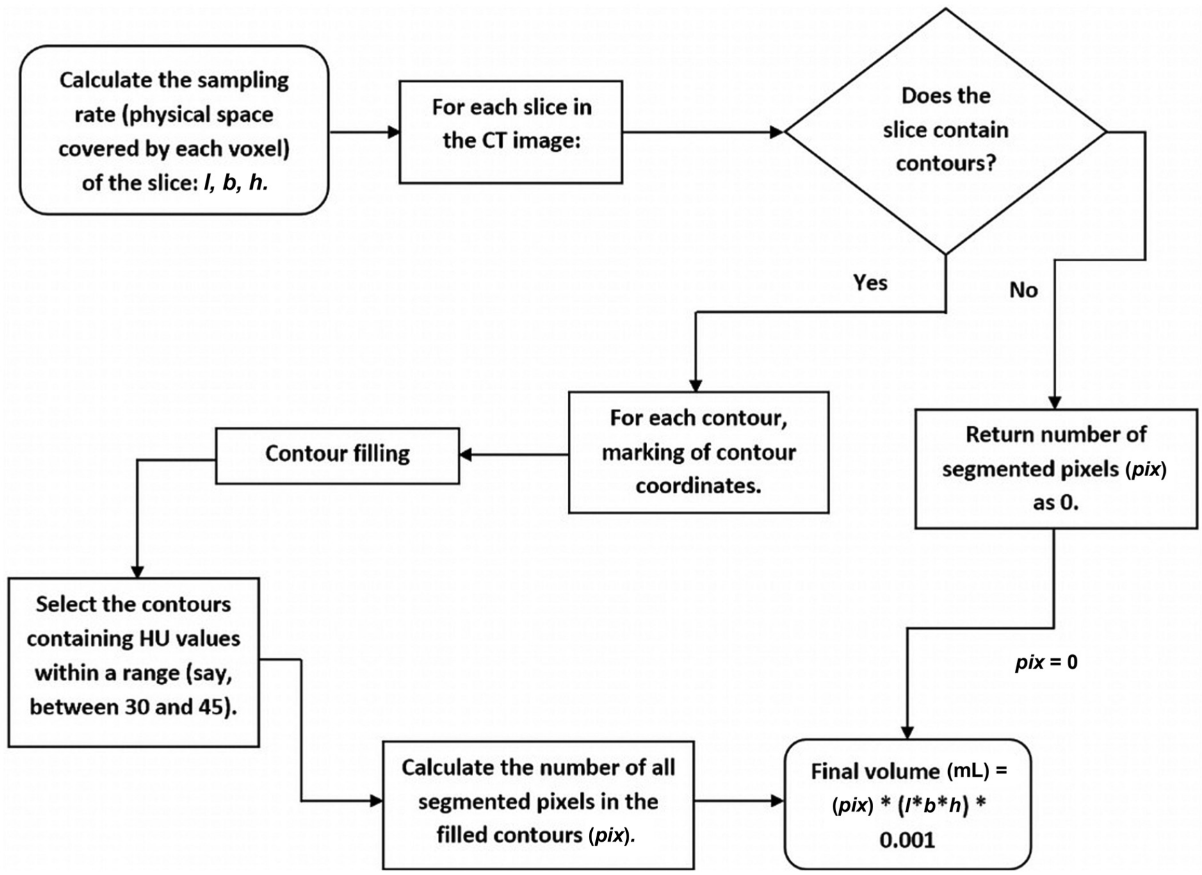

Fig. 4 Segmentation and volume estimation by Contour-Finding and Filling algorithm.

misclassifications and quantification errors. For *HUVAO* to work at its best, it needs a dataset with clear visualizations, precise localization of ROIs, and distinct HU values linked to them. These features work together to accurately identify and isolate ROIs, making the visual assessment process more streamlined. ►**Fig. 7** showcases the separate segmentations of a randomly chosen CT slice with hemoperitoneum, demonstrating how all the algorithms were utilized for segmenting the clinical data.

fig-group>In addressing the potential variability in hemoperitoneum detection based solely on HU values, an exhaustive analysis was conducted within our CT data set. The primary aim was to identify a specific HU value range for consistent and accurate hemoperitoneum segmentation, considering variations influenced by factors like hematocrit and blood age. Individual CT images were meticulously examined to identify common patterns in HU value ranges, supported by reference values provided by the two radiologists' visual estimations. The task involved determining minimum and maximum HU thresholds to minimize volume estimation errors and assessing the practicality of using overlapping HU values for segmentation. The findings emphasize the necessity of a comprehensive strategy for hemoperitoneum detection, acknowledging the limitations of relying solely on HU values in a clinical context. ►**Table 2** summarizes the outcomes of the extensive investigation, exploring lower HU thresholds from 32 to 39 and upper thresholds from 40 to 50, considering all combinations using simple thresholding techniques.

A thorough analysis of the data presented in ►**Table 2** reveals a lack of consistent and accurate estimation of hemoperitoneum volumes through thresholding across the 28 CT scans. The variation in HU thresholds employed for hemoperitoneum segmentation among the scans highlights a lack of uniformity within the data set. This finding emphasizes the inherent difficulties in obtaining precise volume estimates for hemoperitoneum segmentation.

It is essential to note that depending solely on HU values might not be ideal for scenarios involving sensitive medical information. Various factors, such as tissue composition, density, and water content, can impact the HU values of different tissues. Additionally, specific tissues like the liver and spleen can share similar HU values with the hemoperitoneum, making differentiation more challenging. These findings highlight the limitations of image processing algorithms in consistently and accurately segmenting structures in CT scans with overlapping HU regions.

Looking ahead, further research toward refining *HUVAO* and addressing its limitations holds promise. Exploring strategies to enhance the differentiation of tissues with overlapping HU values and refining the algorithm's performance for smaller hemoperitoneum sizes could lead to

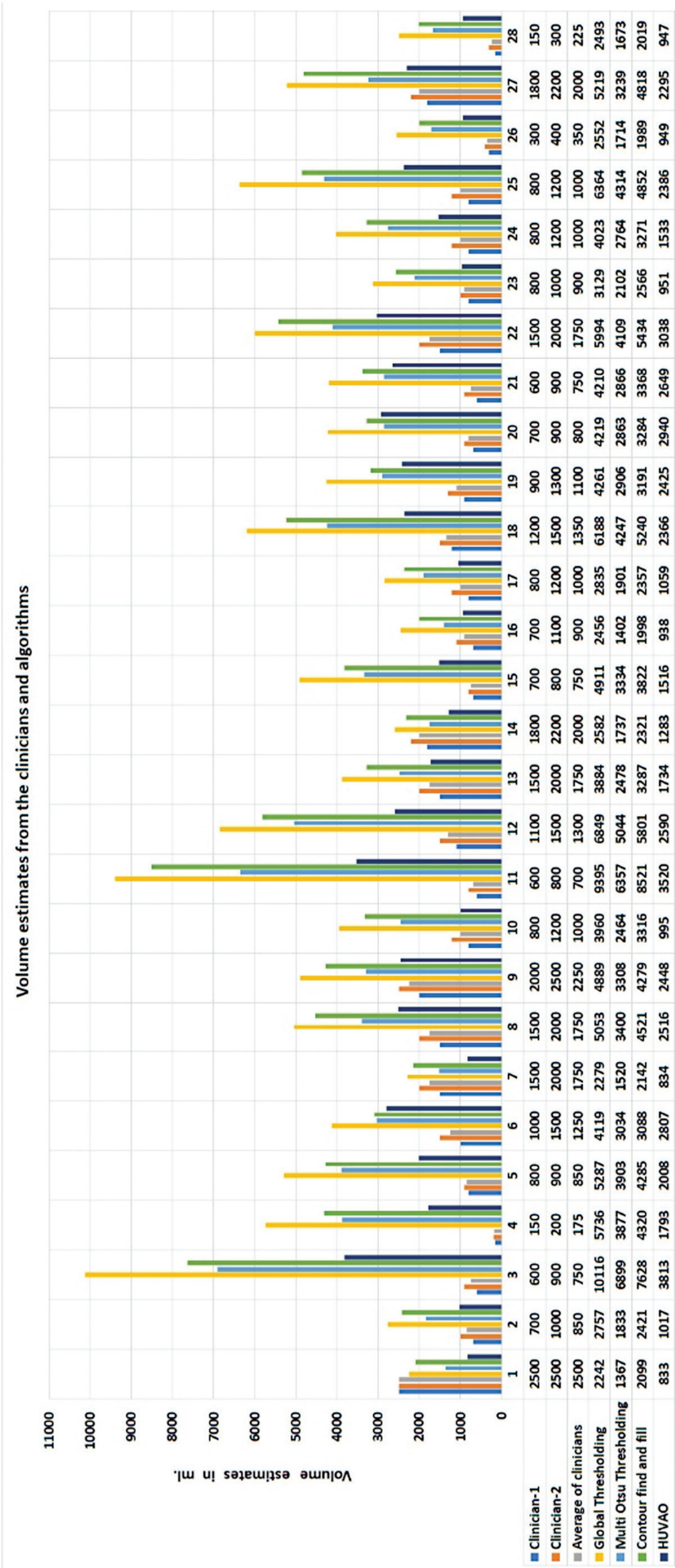

	1	2	3	4	5	6	7	8	9	10	11	12	13	14
Clinician-1	2500	700	600	150	800	1000	1500	1500	2000	800	600	1100	1500	1800
Clinician-2	2500	1000	900	200	900	1500	2000	2000	2500	1200	800	1500	2000	2200
Average of clinicians	2500	850	750	175	850	1250	1750	1750	2250	1000	700	1300	1750	2000
Global Thresholding	2242	2757	10116	5736	5287	4119	2279	5053	4889	3960	9395	6849	3884	2582
Multi Otsu Thresholding	1367	1833	6899	3877	3903	3034	1520	3400	3308	2464	6357	5044	2478	1737
Contour find and fill	2099	2421	7628	4320	4285	3088	2142	4521	4279	3316	8521	5801	3287	2321
HUVAO	833	1017	3813	1793	2008	2807	834	2516	2448	995	3520	2590	1734	1283

	15	16	17	18	19	20	21	22	23	24	25	26	27	28
Clinician-1	700	700	800	1200	900	700	600	1500	800	800	800	300	1800	150
Clinician-2	800	1100	1200	1500	1300	900	900	2000	1000	1200	1200	400	2200	300
Average of clinicians	750	900	1000	1350	1100	800	750	1750	900	1000	1000	350	2000	225
Global Thresholding	4911	2456	2835	6188	4261	4219	4210	5994	3129	4023	6364	2552	5219	2493
Multi Otsu Thresholding	3334	1402	1901	4247	2906	2863	2866	4109	2102	2764	4314	1714	3239	1673
Contour find and fill	3822	1998	2357	5240	3191	3284	3368	5434	2566	3271	4852	1989	4818	2019
HUVAO	1516	938	1059	2366	2425	2940	2649	3038	951	1533	2386	949	2295	947

Fig. 5 Bar graph showing volume estimates obtained from the algorithms as compared with the clinicians' average estimates.

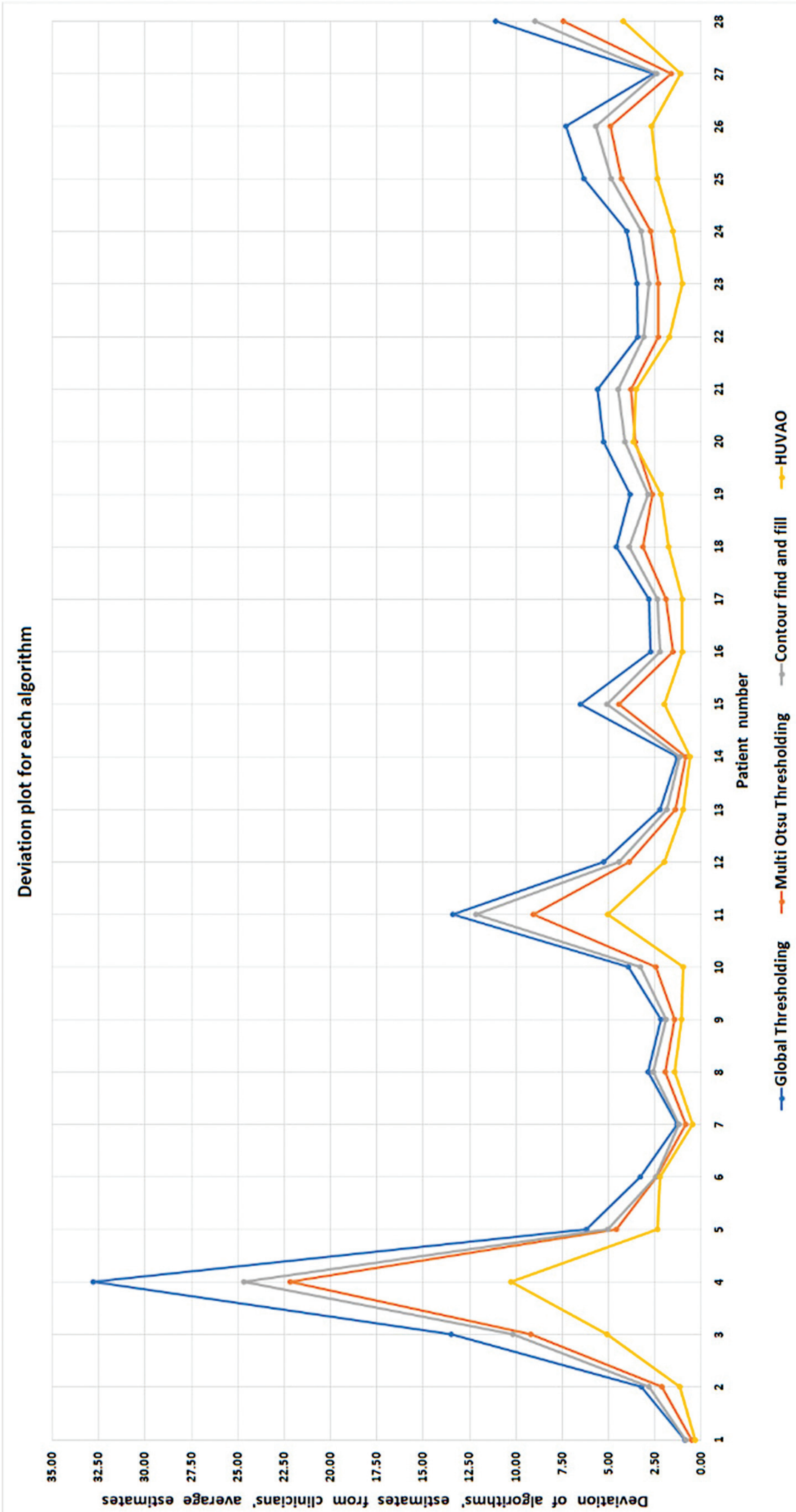

Fig. 6 Deviation plot of the algorithms from the clinicians' average estimates.

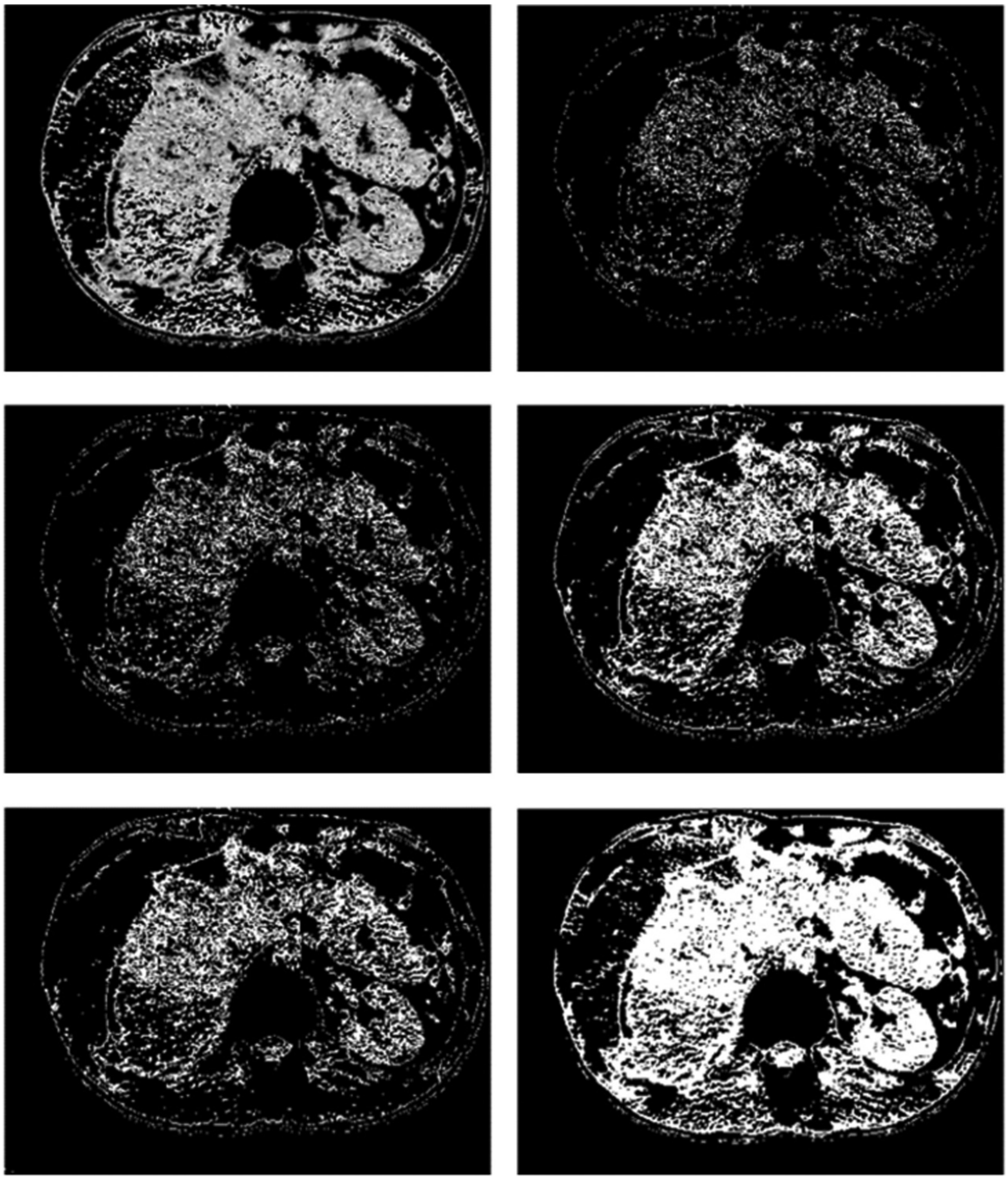

Fig. 7 Hemoperitoneum segmentations: from top: left to right: Cropped and windowed image; Segmentation from an exhaustive search of Hounsfield unit (HU) values to minimize volume estimate error; Segmentation from *HUVAO* (Hounsfield Unit-based Volume quantification of Asymmetrical Objects); Segmentation from Global Thresholding; Segmentation from Multi-Otsu Thresholding; Segmentation from Contour-Finding and Filling algorithm.

improved outcomes. Additionally, investigating the integration of *HUVAO* with advanced technologies, such as deep learning approaches, might offer solutions to the challenges posed by overlapping HU regions. This research direction has the potential to advance the field of medical image processing and contribute to more accurate and reliable diagnoses in complex clinical scenarios.

Conclusion

The subsequent pathways for future investigation are identified based on the findings of our present study, the methodologies implemented, and the resultant outcomes:

(1) The potential approach is to obtain binary annotations for slices containing hemoperitoneum and train a convolutional neural network (CNN) using the annotated data set. The CNN can utilize Class Activation Maps to visually highlight predicted regions within each slice, aiding in further analysis and interpretation.

(2) Another approach involves collaborating with a radiologist to create voxel masks. Neural networks will then be trained to produce probability maps for each slice, simplifying automated pixel identification within the designated voxels. This method has the potential to automate voxel labeling.

Table 2 Exhaustive searching of HU range with minimum HU: [30, 39] and maximum HU: [40, 50] producing the least volume estimate error

Patient. no.	Lower threshold (in HU)	Upper threshold (in HU)	Reference volume (in mL)	Estimated volume (in mL)	Deviation (reference volume/ estimated volume)
1	34	50	2500	2500	1.00
2	36	40	850	867	1.02
3	39	40	750	1330	1.77
4	39	40	175	742	4.24
5	39	40	850	699	0.82
6	36	40	1250	1301	1.04
7	33	44	1750	1753	1.00
8	38	42	1750	1730	0.99
9	36	42	2250	2249	1.00
10	37	40	1000	998	1.00
11	39	40	700	1252	1.79
12	38	40	1300	1341	1.03
13	34	40	1750	1740	0.99
14	33	44	2000	1999	1.00
15	39	40	750	649	0.87
16	39	44	900	916	1.02
17	38	42	1000	982	0.98
18	39	41	1350	1202	0.89
19	39	42	1100	1099	1.00
20	38	40	800	822	1.03
21	38	40	750	809	1.08
22	39	42	1750	1626	0.93
23	39	42	900	864	0.96
24	37	40	1000	1028	1.03
25	39	40	1000	839	0.84
26	39	40	350	341	0.97
27	35	40	2000	1985	0.99
28	39	40	225	329	1.46

Abbreviation: HU, Hounsfield unit.

Contribution to the Knowledge Domain

Our research contributes to and advances our understanding of medical image processing in the context of hemoperitoneum identification and segmentation using non-contrast CT scans. By evaluating a wide array of image processing algorithms, both classical and novel, we shed light on challenges in accurately segmenting structures, especially with overlapping HU regions. We emphasize that relying solely on HU values for blood detection in such cases might yield inconsistent results due to inherent variability influenced by factors like hematocrit, blood age, and contrast agents. Integrating HU values with other modalities and clinical data emerges as essential for precise diagnostics. Our comprehensive exploration reveals the complexities of achieving accurate segmentation within overlapping HU regions. This insight encourages the exploration of advanced techniques like deep learning and combining other methodologies. This knowledge informs the development of improved segmentation modules and promises to enhance diagnostic accuracy and patient care.

Ethical Approval Statement

The present study utilized computed tomography (CT) data sourced from the data archive of the hospital. It is important to note that the data used in this study had previously served to diagnose and treat other medical conditions, making the study inherently retrospective.

Funding
None.

Conflict of Interest
None declared.

Acknowledgments
We acknowledge the Biomechanics and Simulations Laboratory of the Indian Institute of Technology Guwahati for the generous provision of the project's necessary infrastructure and resources. Additionally, we sincerely thank Dr. Meghali Gohain, MD, of the Radiology Department at Apollo Hospital in Guwahati. Dr. Gohain's expertise and contributions were invaluable to our study, providing essential insights and assistance in the field of radiology. We are deeply thankful to our friends and colleagues in the laboratory for their insightful feedback and valuable suggestions throughout the research process.

References

1 ROAD ACCIDENTS IN INDIA 2022. morth.nic.in. Accessed November 16, 2023 at: https://morth.nic.in/sites/default/files/RA_2022_30_Oct.pdf
2 ADSI-2021 | Accidental Deaths & Suicides in India Year Wise. ncrb.gov.in. at: https://ncrb.gov.in/accidental-deaths-suicides-in-india-year-wise.html
3 Sahu MR, Mohanty MK, Sasmal PK, et al. Epidemiology and patterns of road traffic fatalities in India pre- and post-motor vehicle (Amendment) act 2019: an autopsy-based study. Int J Crit Illn Inj Sci 2021;11(04):198–203
4 Road accidents in India - statistics & facts. Statista. Accessed December 26, 2023 at: https://www.statista.com/topics/5982/road-accidents-in-india/
5 Wikipedia Contributors Golden hour (medicine). Wikipedia. Published January 2, 2019. Accessed December 26, 2023 at: https://en.wikipedia.org/wiki/Golden_hour_(medicine)
6 Johnson AB, Waheed A, Burns B Hemorrhage. NIH.gov. Published May 29, 2019. Accessed December 26, 2023 at: https://www.ncbi.nlm.nih.gov/books/NBK542273/
7 Federle MP, Jeffrey RB Jr. Hemoperitoneum studied by computed tomography. Radiology 1983;148(01):187–192
8 Massalou D, Baqué-Juston M, Foti P, Staccini P, Baqué P CT quantification of hemoperitoneum volume in abdominal haemorrhage: a new method. Surg Radiol Anat 2013;35(06):481–486
9 Bloom BA, Gibbons RC. Focused Assessment with Sonography for Trauma. StatPearls [Internet]. Treasure Island, FL: StatPearls Publishing; 2023
10 Rudralingam V, Footitt C, Layton B. Ascites matters. Ultrasound 2017;25(02):69–79
11 UpToDate Published 2020. Accessed December 26, 2023 at: https://www.uptodate.com/contents/initial-evaluation-and-management-of-blunt-abdominal-trauma-in-adults
12 Shanmuganathan K, Mirvis SE, Sover ER. Value of contrast-enhanced CT in detecting active hemorrhage in patients with blunt abdominal or pelvic trauma. AJR Am J Roentgenol 1993;161(01):65–69
13 Diagnostic Ultrasound or CT Scan What's the Difference? Cardiovascular Solutions. Published April 21, 2015. Accessed December 26, 2023 at: http://www.cardiovascularsolutionsinstitute.com/diagnostic-ultrasound-or-ct-scan-whats-the-difference/
14 Wertz JR, Lopez JM, Olson D, Thompson WM. Comparing the diagnostic accuracy of ultrasound and CT in evaluating acute cholecystitis. AJR Am J Roentgenol 2018;211(02):W92–W97
15 Stengel D, Leisterer J, Ferrada P, Ekkernkamp A, Mutze S, Hoenning A. Point-of-care ultrasonography for diagnosing thoracoabdominal injuries in patients with blunt trauma. Cochrane Database Syst Rev 2018;12(12):CD012669
16 DenOtter TD, Schubert J. Hounsfield Unit. Treasure Island, FL: StatPearls Publishing; 2023
17 Kothari RU, Brott T, Broderick JP, et al. The ABCs of measuring intracerebral hemorrhage volumes. Stroke 1996;27(08):1304–1305
18 Huttner HB, Steiner T, Hartmann M, et al. Comparison of ABC/2 estimation technique to computer-assisted planimetric analysis in warfarin-related intracerebral parenchymal hemorrhage. Stroke 2006;37(02):404–408
19 Zhao B, Jia WB, Zhang LY, Wang TZ. 1/2SH: A simple, accurate, and reliable method of calculating the hematoma volume of spontaneous intracerebral hemorrhage. Stroke 2020;51(01):193–201
20 Wikipedia Contributors Cluster analysis. Wikipedia. Published April 20, 2019. Accessed December 26, 2023 at: https://en.wikipedia.org/wiki/Cluster_analysis
21 Clustering in Machine Learning GeeksforGeeks. Published January 15, 2018. Accessed December 26, 2023 at: https://www.geeksforgeeks.org/clustering-in-machine-learning
22 Hojjatoleslami SA, Kittler J. Region growing: a new approach. IEEE Trans Image Process 1998;7(07):1079–1084
23 Adams R, Bischof L. Seeded region growing. IEEE Trans Pattern Anal Mach Intell 1994;16(06):641–647
24 Contour finding—skimage 0.22.0 documentation. Accessed December 26, 2023 at: https://scikit-image.org/docs/table/auto_examples/edges/plot_contours.html
25 Active Contours - A Method for Image Segmentation in Computer Vision Analytics Vidhya. Published September 13, 2021. Accessed December 26, 2023 at: https://www.analyticsvidhya.com/blog/2021/09/active-contours-a-method-for-image-segmentation-in-computer-vision/
26 Hemalatha RJ, Thamizhvani TR, Dhivya AJA, Joseph JE, Babu B, Chandrasekaran R. Active contour based segmentation techniques for medical image analysis. In: Medical and Biological Image Analysis. InTech; 2018
27 Fedorov A, Beichel R, Kalpathy-Cramer J, et al. 3D Slicer as an image computing platform for the Quantitative Imaging Network. Magn Reson Imaging 2012;30(09):1323–1341
28 Hillal A, Sultani G, Ramgren B, Norrving B, Wassélius J, Ullberg T. Accuracy of automated intracerebral hemorrhage volume measurement on non-contrast computed tomography: a Swedish Stroke Register cohort study. Neuroradiology 2023;65(03):479–488
29 Wu TY, Sobowale O, Hurford R, et al. Software output from semi-automated planimetry can underestimate intracerebral haemorrhage and peri-haematomal oedema volumes by up to 41. Neuroradiology 2016;58(09):867–876
30 Freeman WD, Barrett KM, Bestic JM, Meschia JF, Broderick DF, Brott TG. Computer-assisted volumetric analysis compared with ABC/2 method for assessing warfarin-related intracranial hemorrhage volumes. Neurocrit Care 2008;9(03):307–312
31 Haley MD, Gregson BA, Mould WA, Hanley DF, Mendelow AD. Retrospective methods analysis of semiautomated intracerebral hemorrhage volume quantification from a selection of the STICH II cohort (Early Surgery Versus Initial Conservative Treatment in Patients With Spontaneous Supratentorial Lobar Intracerebral Haematomas). Stroke 2018;49(02):325–332
32 Osiri X DICOM Viewer | Technical Sheet. Accessed December 26, 2023 at: https://www.osirix-viewer.com/resources/technical-sheet
33 Battey TWK, Dreizin D, Bodanapally UK, et al. A comparison of segmented abdominopelvic fluid volumes with conventional CT signs of abdominal compartment syndrome in a trauma population. Abdom Radiol (NY) 2019;44(07):2648–2655
34 Chen M, Li Z, Ding J, Lu X, Cheng Y, Lin J. Comparison of common methods for precision volume measurement of hematoma. Comput Math Methods Med 2020;2020:6930836

35 Dreizin D, Zhou Y, Zhang Y, Tirada N, Yuille AL. Performance of a deep learning algorithm for automated segmentation and quantification of traumatic pelvic hematomas on CT. J Digit Imaging 2020;33(01):243–251
36 Dreizin D, Bodanapally UK, Neerchal N, Tirada N, Patlas M, Herskovits E. Volumetric analysis of pelvic hematomas after blunt trauma using semi-automated seeded region growing segmentation: a method validation study. Abdom Radiol (NY) 2016;41(11): 2203–2208
37 Lee JY, Kim JS, Kim TY, Kim YS. Detection and classification of intracranial haemorrhage on CT images using a novel deep-learning algorithm. Sci Rep 2020;10(01):20546
38 Dreizin D, Nixon B, Hu J, et al. A pilot study of deep learning-based CT volumetry for traumatic hemothorax. Emerg Radiol 2022;29 (06):995–1002
39 Sabour S. Interrater reliability among radiologists reading PET/contrast-enhanced CT scans using NI-RADS: methodologic issues. Radiol Imaging Cancer 2021;3(05):e210062
40 Blake KE, Beffa LR, Petro CC, Krpata DM, Prabhu AS, Rosen MJ. Surgeon accuracy and interrater reliability when interpreting CT scans after ventral hernia repair. Hernia 2023;27(02):347–351
41 Bechstein M, McDonough R, Fiehler J, et al. Radiological evaluation criteria for chronic subdural hematomas: review of the literature. Clin Neuroradiol 2022;32(04):923–929
42 Yan JL, Chen YL, Chen MY, et al. A robust, fully automatic detection method and calculation technique of midline shift in intracranial hemorrhage and its clinical application. Diagnostics (Basel) 2022; 12(03):693
43 Furlan A, Fakhran S, Federle MP. Spontaneous abdominal hemorrhage: causes, CT findings, and clinical implications. AJR Am J Roentgenol 2009;193(04):1077–1087
44 Levine CD, Patel UJ, Silverman PM, Wachsberg RH. Low attenuation of acute traumatic hemoperitoneum on CT scans. AJR Am J Roentgenol 1996;166(05):1089–1093
45 Ahn JH, Yoo DG, Choi SJ, et al. Hemoperitoneum caused by hepatic necrosis and rupture following a snakebite: a case report with rare CT findings and successful embolization. Korean J Radiol 2007;8(06):556–560
46 Maxime St-Amant Hemoperitoneum | Radiology Reference Article | Radiopaedia.org. Radiopaedia.org. Published 2012. Accessed November 17, 2023 at: https://radiopaedia.org/articles/haemoperitoneum
47 Robinson JD, Sandstrom CK, Lehnert BE, Gross JA. Imaging of blunt abdominal solid organ trauma. Semin Roentgenol 2016;51(03): 215–229. Doi: 10.1053/j.ro.2015.12.003
48 Gayer G, Hertz M, Manor H, Strauss S, Klinowski E, Zissin R. Dense ascites: CT manifestations and clinical implications. Emerg Radiol 2004;10(05):262–267
49 Lee MS, Moon MH, Woo H, Sung CK, Jeon HW, Lee TS. Ruptured corpus luteal cyst: prediction of clinical outcomes with CT. Korean J Radiol 2017;18(04):607–614
50 Rogowska J. Overview and fundamentals of medical image segmentation. In: Handbook of Medical Imaging. Elsevier; 2000:69–85
51 Davies ER. Thresholding Techniques. In: Computer and Machine Vision. Elsevier; 2012:82–110
52 Abera KA, Manahiloh KN, Motalleb Nejad M. The effectiveness of global thresholding techniques in segmenting two-phase porous media. Constr Build Mater 2017;142:256–267
53 Multi-Otsu Thresholding—skimage v0.19.2 docs. scikit-image.org. Accessed December 26, 2023 at: https://scikit-image.org/docs/stable/auto_examples/segmentation/plot_multiotsu.html
54 Zhang P, Lu S, Li J, et al. Multi-component segmentation of X-ray computed tomography (CT) image using multi-Otsu thresholding algorithm and scanning electron microscopy. Energy Explor Exploit 2017;35(03):281–294
55 Skimage.Filters—skimage 0.22.0 documentation. Scikit-image.org. Accessed November 16, 2023 at: https://scikit-image.org/docs/stable/api/skimage.filters.html

